Наносистеми, наноматеріали, нанотехнології
Nanosistemi, Nanomateriali, Nanotehnologii
2025, т. 23, № 3, сс. 879–894
https://doi.org/10.15407/nnn.23.03.0879

PACS numbers: 06.60.Vz, 61.05.cp, 62.20.Qp, 62.23.Pq, 68.37.Hk, 81.20.Ev, 81.40.Pq

Si_3N_4–TiN Wear-Resistant Composite Ceramics with a Surface Layer of 2*D* MoSSe Nanostructures

R. V. Lytvyn[1], N. B. Konih-Ettel[1], I. A. Poliakov[1], I. V. Kud[1], O. M. Myslyvchenko[1], V. G. Kolesnichenko[1], O. M. Postrelko[1], L. M. Kulikov[1], M. Yu. Barabash[2,3,4,5], and O. B. Zgalat-Lozynskyy[1]

[1]*I. M. Frantsevych Institute for Problems of Materials Sciences, N.A.S. of Ukraine, 3, Omeljan Pritsak Str., UA-03142 Kyiv Ukraine*
[2]*Technical Centre, N.A.S. of Ukraine, 13, Pokrovs'ka Str., UA-04070 Kyiv, Ukraine*
[3]*National Technical University of Ukraine 'Igor Sikorsky Kyiv Polytechnic Institute', 37, Beresteiskyi Ave., UA-03056 Kyiv, Ukraine*
[4]*Gas Institute, N.A.S. of Ukraine, 39, Degtyarivska Str., UA-03113 Kyiv, Ukraine*
[5]*Institute for Applied Control Systems, N.A.S. of Ukraine, 42, Academician Hlushkov Ave., UA-03187 Kyiv, Ukraine*

The paper presents the results of the development and tribological evaluation of a system based on Si_3N_4–25 wt.% TiN composite ceramic with a surface layer of solid lubricant composed of substitutional solid solution of 2*D* MoSSe (molybdenum sulphoselenide) nanostructures. The Si_3N_4–TiN composite powder is synthesized by thermal reaction of precursors. Dense ceramic specimens with a relative density of 0.98 and a microhardness of 15.7 GPa are fabricated by spark plasma sintering at a maximum temperature of 1800°C. 2*D* MoSSe nanostructures are synthesized by chemical vapour deposition. A solid lubricant layer of 2*D* MoSSe nanostructures is deposited on the surface of the ceramic specimens by ultrasound-assisted deposition in ethanol, followed by drying and annealing at 200°C. Tribological tests are performed under dry sliding and with a solid lubricant layer according to the ball-on-disk scheme in contact with ceramic and steel counterbodies. As shown, the presence of 2*D* MoSSe reduces significantly the friction force and linear wear: for the ceramic counterbody, linear wear decreases by a factor of 10–20 depending on the loading re-

gime. The friction force in the tribosystem with the solid lubricant, as compared to that under dry sliding, decreases by a factor of 2–6 for the steel indenter under dynamic-loading conditions and by a factor of 2–10 for the ceramic indenter, depending on the sliding time. The SEM and EDS data confirm the formation of a dense tribolayer based on 2*D* MoSSe. This layer reduces the adhesive and abrasive wear under friction in the ceramic–lubricant–steel tribosystem. The obtained results create prerequisites for using developed materials in hybrid bearings and other friction units operating under extreme conditions.

В роботі представлено результати дослідження з розробки та триботестування системи з композиційної кераміки складу Si_3N_4–25 мас.% TiN із поверхневим шаром твердого мастильного матеріялу з нанокристалічного порошку твердого розчину заміщення сульфідоселеніду Молібдену 2*D*-MoSSe. Композиційний порошок Si_3N_4–TiN одержано термічною синтезою з прекурсорів. Компактні керамічні зразки із густиною у 0,98 від теоретичної та мікротвердістю у 15,7 ГПа виготовлено методом іскроплазмового спікання за максимальної температури у 1800°C. Наноструктури 2*D*-MoSSe синтезовано методом хемічного осадження з парової фази. Шар твердого мастила з наноструктур 2*D*-MoSSe нанесено на поверхню керамічних зразків методом ультразвукового осадження в етилені з наступною сушкою та відпалом за температури у 200°C. Проведено триботести в умовах сухого тертя та з шаром твердого мастила за схемою площина–куля у контакті з керамічним і крицевим контртілами. Показано, що присутність 2*D*-MoSSe істотно понижує силу тертя та лінійний знос: у парі з керамічним контртілом лінійний знос зменшується у 10–20 разів залежно від режиму навантаження. У порівнянні з сухим тертям сила тертя в трибосистемі з твердим мастилом зменшується для крицевого індентора за динамічних умов навантаження в 2–6 разів, для керамічного індентора — в 2–10 разів в залежності від тривалости тертя. За даними сканувальної електронної мікроскопії та енергодисперсійної рентґенівської спектроскопії у трибосистемі кераміка–мастильний шар–крицеве контртіло утворюється щільний трибошар на основі 2*D*-MoSSe, який сприяє пониженню адгезійного й абразивного зношування під час тертя. Одержані результати створюють передумови для застосування розроблених матеріялів у гібридних вальницях та інших вузлах тертя, що працюють в екстремальних умовах.

Key words: composite ceramic, Si_3N_4, TiN, spark plasma sintering, solid lubricant, 2*D* nanostructures, MoSSe, wear resistance.

Ключові слова: композиційна кераміка, Si_3N_4, TiN, іскроплазмове спікання, тверде мастило, 2*D*-наноструктури, MoSSe, зносостійкість.

(Received 16 July, 2025)

1. INTRODUCTION

In Ukraine, the technical ceramic market actively developed until

2022, and now, in wartime with import restrictions, its rapid growth is expected. The most promising directions for the import substitution of components of critical import are the productions of wear-resistant composites and modern lubricants for operation under extreme conditions. Wear-resistant ceramics for operation under conditions of high loads and temperatures are traditionally manufactured from silicon nitride, but to increase substantially the wear resistance, it is necessary to select friction couples and a lubricant that corresponds to the operating conditions. In the production of hybrid bearings with balls based on silicon nitride, as the second material of the friction couple, components based on steel are used [1–3]. Unfortunately, in most cases, the operation of a ceramic–steel couple under extreme conditions is limited by the rapid wear of steel components [4–8]. In this connection, the search for new friction couples for ceramic materials based on silicon nitride, the development of efficient lubricants, and the determination of functioning regularities of friction couples depending on the physicomechanical characteristics of the materials of tribological conjunctions is an urgent problem.

The structure and composition of wear-resistant composites based on silicon nitride substantially influence their tribological and mechanical properties. Researchers of modern wear-resistant ceramics are giving most attention to the determination of the influence of the composition of materials based on silicon nitride and the size of structural elements [8–15]. The structural factor (grain size and porosity), as a rule, depends on the chosen consolidation method of the wear-resistant composite. For instance, in Ref. [8], tribotests of counterbodies made of commercial silicon nitride powder with a grain size above 1 μm were carried out according to the 'ball-on-disk' scheme under condition of marginal lubrication and dry friction. An analysis of the obtained data showed that the tribological properties of silicon nitride substantially increased as a result of imparting nanostructuring to it. However, at the same time, the fracture toughness of such ceramics substantially decreases, which limits the field of application of nanocrystalline wear-resistant ceramics based on silicon nitride. The tribological properties can be improved by introducing titanium nitride into the composition [8, 10, 12, 14, 15]. As compared to monolithic Si_3N_4 ceramics, Si_3N_4–TiN composites demonstrate a higher wear resistance and a smaller coefficient of friction. At the same time, the mechanical properties of ceramic composites based on silicon nitride can be improved by the formation of a bimodal granular structure [10, 12].

One way of solving the problem of improving the functional characteristics of wear-resistant ceramics is to achieve a macroscale super lubricating ability of materials to minimize friction, in par-

ticular by using two-dimensional (2*D*) materials [16–20]. Due to the weak interlayer interaction, 2*D* materials have the potential to achieve the superlubrication effect. Most investigations are devoted to graphene-like monolayers and nanoparticles ('few-layers') of layered *d*-transition metal dichalcogenides, which are 2*D* inorganic analogues of graphene, and to their numerous nanoheterostructures (van der Waals nanostructures) [20]. Among these, molybdenum disulphide with the 2*H*-MoS_2 structure type and materials based on carbon (including graphite and graphene) are best studied [20, 21]. At present, micron powders of natural MoS_2 with a layered structure are successfully used in industrial scales as efficient solid lubricants and are components of numerous antifriction materials (industrial lubricants, oils, greases, and coatings) due to the relatively widespread availability of commercial micron powders of MoS_2 of natural origin. In practice, solid lubricant additives to oils and greases are successfully used only an in the case of very small particle size that makes it possible to stabilize their suspension and prevent the deposition of lubrication systems on filters. Another limitation to using MoS_2–steel friction systems is the formation of iron sulphide (FeS_2) or solid iron solutions in molybdenum disulphide, which is accompanied by the fracture of the surface of steel structural elements and an unpredictable change in the properties of the lubricant [22]. A possible way of solving this problem is to reduce the sulphur content, in particular to replace sulphur by selenium by the method of using substitutional solid solutions 2*D* $MoS_{2-x}Se_x$ ($0 \le x \le 2$), which will kinetically limit the formation of undesirable FeS_2. For instance, the use of nanopowders of 2*D* $MoS_{2-x}Se_x$ ($0 \le x \le 2$) substitutional solid solutions as a solid lubricant or additives to lubricants or oils is a promising direction of improving the operation of hybrid or other friction units.

Wear-resistant materials for the transport, machine building, chemical, and aerospace industries often operate under extreme conditions of high or ultralow temperature and high pressure, which leads to their intensive wear. The use of a lubrication system based on nanopowders of 2*D* $MoS_{2-x}Se_x$ ($0 \le x \le 2$) substitutional solid solutions in combination with the components of tribological conjunctions of the composite nanoceramic will favour an increase in the service life of machines and mechanisms and the assurance of high energy efficiency indices.

Thus, the aim of the work is to investigate the preparation conditions of Si_3N_4–TiN wear-resistant composite materials, deposit of solid lubricant layer from substitutional solid solution of molybdenum sulphide selenide 2*D* $MoS_{2-x}Se_x$ ($x = 1$) nanostructures, and determine the tribological characteristics of the obtained tribosystem in friction couples with a ceramic and a steel counterbody.

2. INITIAL MATERIALS AND EXPERIMENTAL TECHNIQUES

The initial material for the manufacture of composites was a 75 mass% Si_3N_4 + 25 mass% TiN powder mixture (corresponds to a volume content of titanium nitride of 17%), which was obtained by the synthesis technology developed in the IPMS N.A.S.U. and described in Refs. [23, 24]. This technology assumes the use of commercial silicon nitride and titanium powders, which are available in the Ukrainian market as precursors. The micron Si_3N_4 powder (DZKhR LLC, Ukraine) and titanium powder with a mean particle size of 0.5 mm ('Velta' Mining Company, Ukraine) were subjected to mechanical mixing to reduce the powder particle size and provide a homogeneous distribution of the components. Mixing was performed in a Pulverisette 6 planetary mill (Fritch GmbH, Germany) in ethanol using a drum and milling balls made of silicon nitride at a rotational speed of 400 rpm and a ball-to-powder weight ratio of 4:1 for 5 h. The prepared mixture was subjected to heat treatment in an SNV–1.3,1/20–I1 high-temperature electric furnace in the temperature range of 1100–1400°C in a vacuum of $\cong 1 \cdot 10^{-3}$ Pa and in a nitrogen atmosphere to synthesize Si_3N_4–25 mass% TiN composite powder.

Spark plasma sintering (SPS) was carried out in a FCT HP D25 furnace (Systeme GmbH, Germany) in a graphite die with a diameter of 20 mm in a nitrogen atmosphere at maximum temperature of 1800°C, maximum pressure $P = 30–50$ MPa, and heating rate of 70–100°C/min. Aluminium and yttrium oxides in amounts of 5 mass% and 6 mass%, respectively, were added to the synthesized powder to intensify densification in sintering. Sintering regimes were chosen on the basis of information about densification of powder compositions [25] to achieve a maximum density. The change in the linear size of specimens was evaluated from the displacement of the upper punch at a stationary lower punch.

The nanocrystalline powder of the substitutional solid solution 2*D* $MoS_{2-x}Se_x$ ($x = 1$, in what follows, MoSSe) was synthesized by the chemical vapour deposition method (CVD) at the interaction of the constituent elements (MPCh high-purity molybdenum powder, elemental sulphur and selenium powders of more than 99.9% purity in stoichiometric ratios Mo:S:Se = 1:1:1 in evacuated quartz ampoules in modes tested by the authors under laboratory conditions [26].

The x-ray analysis of the synthesized 2*D* MoSSe nanostructures was carried out on an HZG-4A automated powder diffractometer in FeK_α-radiation by full-profile method, including the determination of the average sizes of anisotropic nanoparticles. The indexing of XRD patterns, the refinement of the parameters of elementary cells by the least square method (LSM) and structural parameters were

performed by the WinCSD software for structural calculations [27]. The average sizes of anisotropic nanoparticles were determined by the method of line broadening analysis (Scherrer formula). In the analysis of the functions of physical expansion, the possible distortions of the crystal structure (Stokes formula) was taken into account. Corresponding computer calculations of the nanoparticles' average sizes in the crystallographic directions [013] and [110] were performed with the help of the improved WinCSD [27].

The surface of sintered ceramic Si_3N_4–TiN specimens was covered by 2*D* MoSSe nanostructures as lubricant coating by deposition after ultrasonic treatment (cavitation mode) for 1 h in ethanol. After deposition, the obtained specimens were air-dried at room temperature and annealed in the air at 200°C for 3.5 h. The thickness of coating 2*D* MoSSe was estimated to be of about 17 μm by gravimetric method.

SEM analysis was performed with Mira 3 scanning electron microscope (Tescan, Czech Republic).

The friction and wear parameters of a ceramic Si_3N_4–TiN specimen were investigated at room temperature on an automated tribodynamic complex (ATKD) with a module of dynamic loading in the quasi-stationary and dynamic operating modes [15]. Tribological tests were carried out according to the plane–ball scheme in couples with counterbodies, namely a ceramic (Si_3N_4) or a steel (ShKh-15) ball 8 mm in diameter [28–31]. Wear tests of a clean surface of the Si_3N_4–TiN ceramic and a ceramic surface after deposition of a lubricant layer from the 2*D* MoSSe nanopowder on it were carried out. The mean sliding speed was of 1.47 mm/s. This value was chosen to model microsliding in ball bearings operating at a speed of $\cong$ 105 rpm [32]. The test time was chosen equal to 30 min to provide a stable friction mode. The tests included static and dynamic loading. Dynamic loading combines the action of a static load of 30 N and an oscillating load with amplitude of 4.5 N and a frequency of 25 Hz, which modulates oscillations of the load in ball bearings [5]. The parameters of tribotechnical tests were chosen on the basis of results of previous investigation of similar composite materials based on silicon nitride [6–8, 15]. The combination of the static and dynamic loading makes it possible to investigate the contribution of different mechanisms into wear processes. It has been previously shown on a large series of materials (from aluminium alloys to ceramics) that dynamic loading reduces the force of friction and the adhesive component of wear, but can increase wear, when its main mechanism is fatigue or abrasive wear [5–8, 29–33]. In tribotests, the friction force, the size of the contact spot, and linear wear were determined from the profile of the tribocontact zone. The system for measuring the friction force consists of a calibrated elastic ele-

ment sensitive to an inductive displacement sensor and a 12-bit analog-to-digital converter [15]. Wear was measured on a Leeb 462 surface roughness tester.

3. RESULTS AND DISCUSSION

3.1. Si_3N_4–TiN Ceramic Material

For the sintering of ceramic specimens, the composite powder based on silicon nitride and obtained by thermal synthesis from precursors was used. According to the XRD data, it contains 83 mass% Si_3N_4 and 25 mass% TiN (Fig. 1).

According to data of the SEM and EDS analyses, the synthesis product is a highly disperse composite powder containing TiN (light phase **B**) and β-Si_3N_4 (dark phase **A**) (Fig. 2) in the form of a mixture of agglomerates of titanium nitride particles with a size of 30–200 nm in the β-Si_3N_4 matrix. Before sintering, the powder was subjected to deagglomeration in the Pulverisette 6 planetary mill to homogenize the distribution of the components.

As a result of spark plasma sintering of the composite Si_3N_4–TiN powder, dense specimens of cylindrical shape were obtained. The analysis of the densification data of a specimens showed that, in the temperature range of 700–900°C, a negative shrinkage took place as a result of the thermal expansion of the graphite die. Intensive densification begins at a temperature of ≅ 1350°C, which can be associated with the formation of a eutectic liquid phase in the SiO_2–Al_2O_3–Y_2O_3 system. A maximum densification rate of ≅ 1.6 mm/min is attained at ≅ 1470°C, which agrees with analogous data for composite materials containing nanodisperse titanium nitride particles

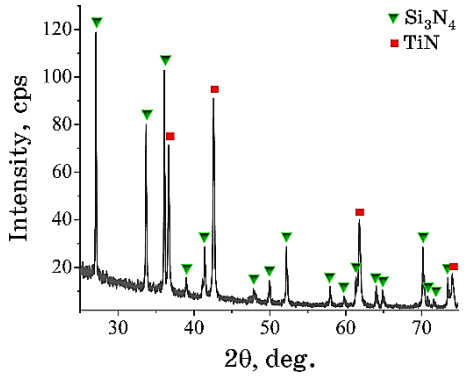

Fig. 1. X-ray diffraction pattern of the Si_3N_4–25 mass% TiN composite powder.

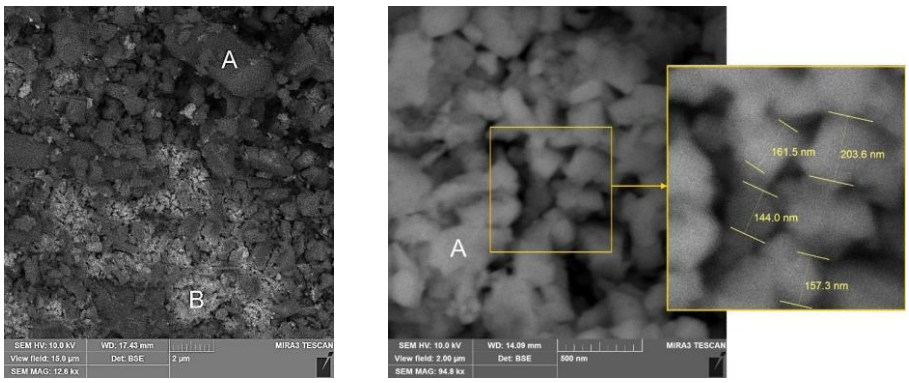

Fig. 2. SEM image of the synthesized composite powder (**A**—Si_3N_4, **B**—TiN): *a*—general view; *b*—region with a dominant titanium nitride content.

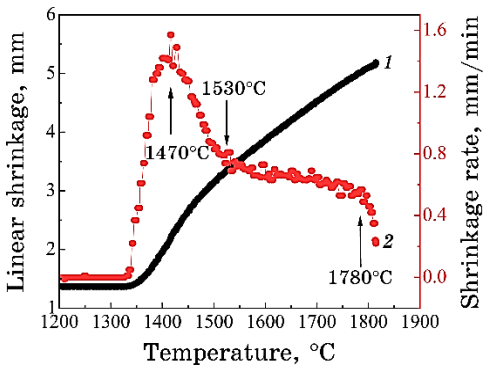

Fig. 3. Temperature dependence of densification parameters in the SPS process: *1*—linear shrinkage of the specimen; *2*—densification rate.

[10, 34] (Fig. 3). Then, the densification rate decreases down to 0.6–0.8 mm/min and remains constant in the temperature range of 1530–1780°C.

The analysis of the microstructure of the Si_3N_4–TiN composite consolidated by SPS showed zonal isolation with the formation of regions of predominant content of titanium nitride grains (Fig. 4). Moreover, acicular silicon nitride grains are observed, which is characteristic of sintering with the formation of a liquid phase after attainment of high temperatures.

On the whole, the structure of the Si_3N_4–TiN composite is bimodal, where silicon nitride grains with a size up to several microns as well as titanium nitride and silicon nitride grains with a size of

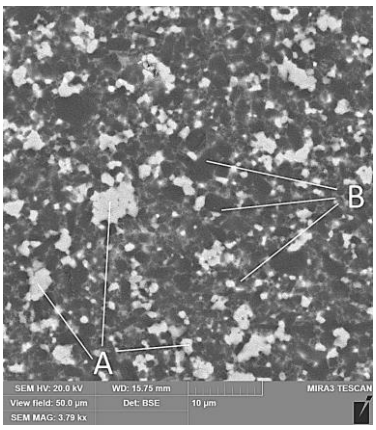

Fig. 4. SEM image of the Si_3N_4–TiN ceramic sintered by the SPS at temperature of 1800°C: **A**—TiN, **B**—Si_3N_4.

200–500 nm are present. The specimens of the Si_3N_4–TiN composite material sintered at 1800°C had a relative density of 98% and a microhardness of 15.7 ± 0.8 GPa.

3.2. Analysis of the Synthesized 2*D* MoSSe Nanostructures

It was established by x-ray data that the synthesized anisotropic 2*D* MoSSe nanostructures were homogeneous in chemical composition, with type of the layered structure (2*H*-MoS_2) and the type of nanostructures (2*D*, few-layers nanosheets), did not contain foreign impurities, including roentgen-amorphous impurities, phases, and other nanostructures, as well as micron particles. The average sizes of 2*D* MoSSe nanoparticles in the crystallographic direction [013] and [110] are $d_{[013]} = 4.9(3)$ nm and $d_{[110]} = 22.6(1)$ nm, respectively; the parameters of the elementary cell of 2*D* MoSSe are $a = 0.3209(1)$ nm and $c = 1.2637(7)$ nm.

According to SEM data analysis, the synthesized 2*D* MoSSe nanoparticles have clear facets (hexagons form) that testifies to the stationarity of the physicochemical conditions of their growth. The nanoparticles form agglomerates as a result of the action of common crystallization centres in the initial stage of the growth process (Fig. 5).

3.3. Tribological Characteristics of Ceramic–Ceramic and Ceramic–Metal Friction Couples with 2*D* MoSSe Solid Lubricant

The surface of sintered ceramic Si_3N_4–TiN specimens was covered

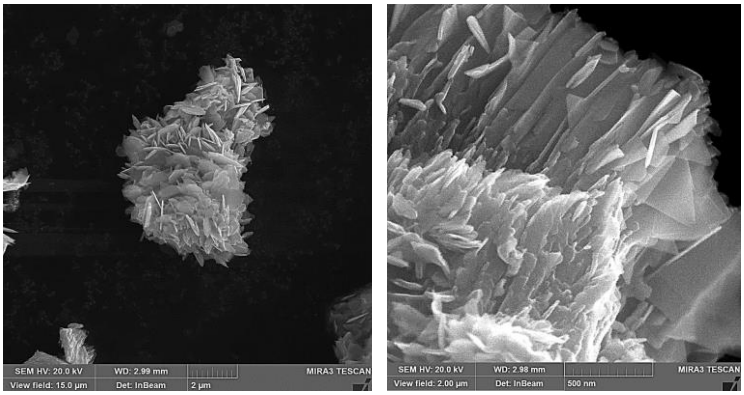

a *b*

Fig. 5. SEM images of agglomerated 2*D* MoSSe nanoparticles in view field of: *a*—15 µm, *b*—2 µm.

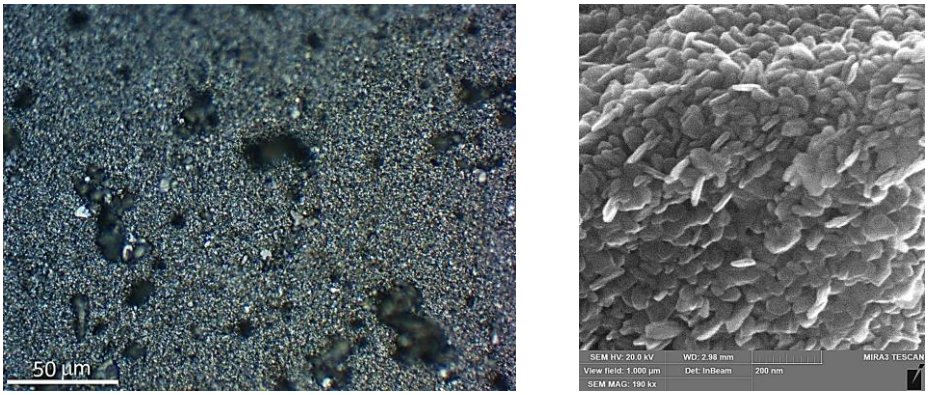

a *b*

Fig. 6. The surface of the ceramic specimen covered with 2*D* MoSSe solid lubricant: *a*—optical image in view field of 200 µm; *b*—SEM image in view field of 1 µm.

by 2*D* MoSSe nanostructures as lubricant coating to reduce the shear resistance in the region of tribocontact and friction coefficient (Fig. 6).

The adhesion strength of the coating and its influence on the tribotechnical indices depend on the initial state of the surface of the sintered ceramic material and its mechanical properties. The fact that sliding with a low shear resistance in MoSSe favours a decrease in friction and wear is undeniable. Micrographs of worn surfaces demonstrate that the presence of the MoSSe lubricant layer leads to the formation of a tribolayer in the tribocontact zone in the cases of

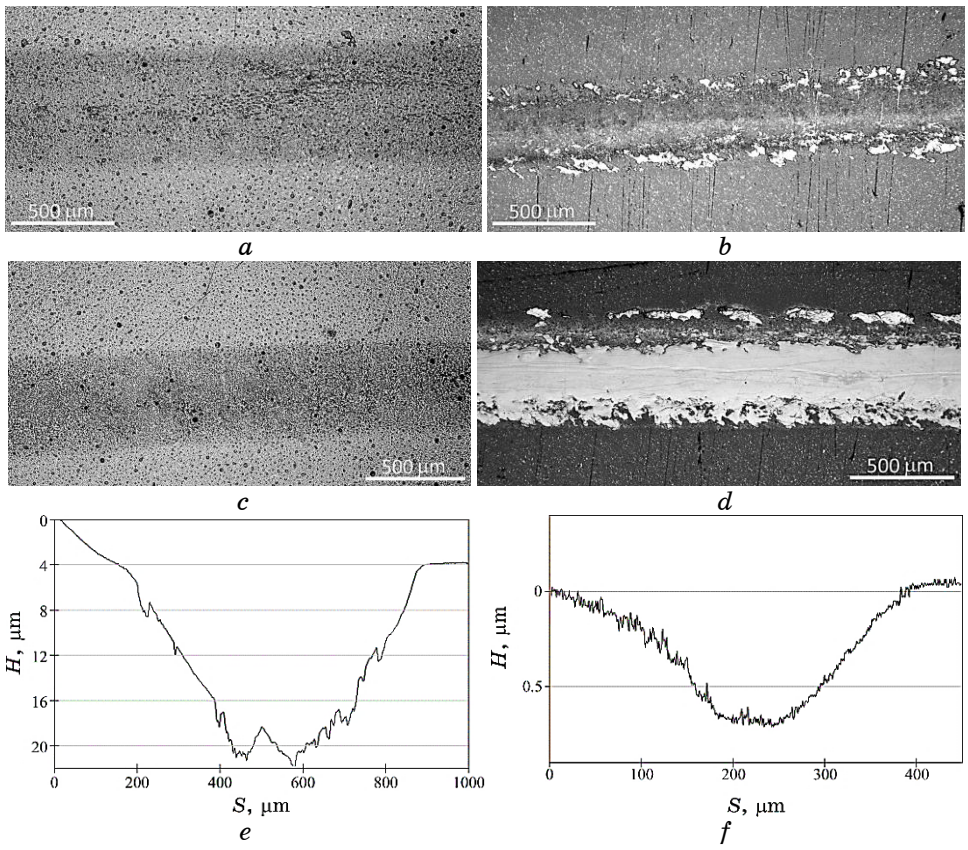

Fig. 7. Tribocontact surface on sintered Si_3N_4–TiN specimens: *a*—with ceramic counterbody; *b*—with ceramic counterbody and 2*D* MoSSe solid lubricant; *c*—with steel counterbody; *d*—with steel counterbody and 2*D* MoSSe solid lubricant; *e*—surface profile of friction zone with ceramic counterbody; *f*—surface profile of friction zone with ceramic counterbody and 2*D* MoSSe solid lubricant.

both the steel and the ceramic counterbody (Fig. 7, *b*, *d*).

The morphology of the tribolayer changed depending on the material of the counterbody and the type of loading (static or dynamic). Under dynamic loading, an almost continuous surface layer formed for the ShKh15 counterbody (Fig. 7, *d*). For the ceramic counterbody, the formed layer was fragmented but sufficiently dense to influence the obtained results (Fig. 7, *b*).

According to the EDS data, the tribolayer consists of Mo, S, Se, and the material of the counterbody. In friction without lubricant, a tribolayer did not form (Figs. 7, *a*, *c*), which led to the intensive wear and damage of the surface. In the presence of 2*D* MoSSe coat-

ing, a noticeable damage of the surface of the ceramic material did not occur, which confirms the efficiency of the used approach for decreasing the adhesive interaction between solid surfaces during tribocontact.

A substantial decrease in the wear after introduction of the MoSSe solid lubricant into the tribocontact zone was detected also by the analysis of the tribocontact surface profile (Figs. 7, *e*, *f*). The presence of solid lubricant nanostructures abruptly decreases the linear wear of the surface specimen in the couple with a ceramic indenter, namely by a factor of 20 under static conditions and by a factor of 10–11 under conditions of dynamic loading (Fig. 8). A significant reduction in linear wear of the steel counterbody lubricated with MoSSe compared to dry sliding was observed; however, its reliable quantification was complicated by the presence of a dense tribolayer. Additionally, a decrease in the friction force under dynamic loading conditions was recorded, amounting to 2–6-fold

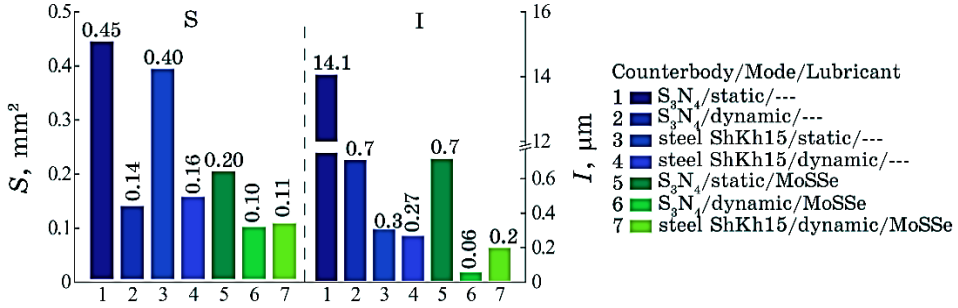

Fig. 8. Area of the contact spot (*S*) and the linear wear (*I*) of the Si_3N_4–TiN composite material before and after deposition of the 2*D* MoSSe solid lubricant.

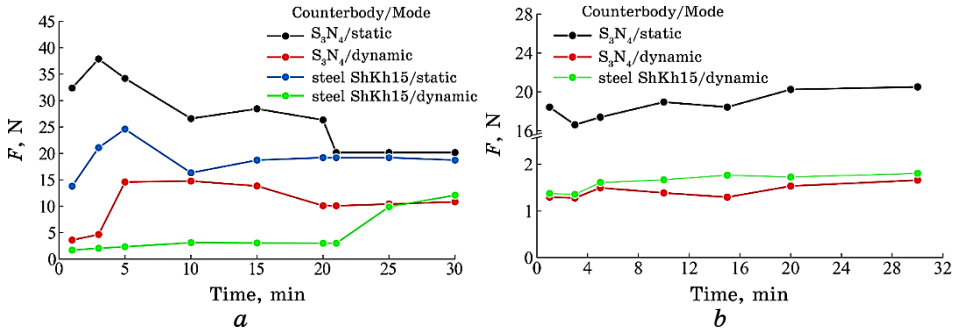

Fig. 9. Friction force (*F*) on the Si_3N_4–TiN surface: *a*—dry friction, *b*—friction with the 2*D* MoSSe solid lubricant.

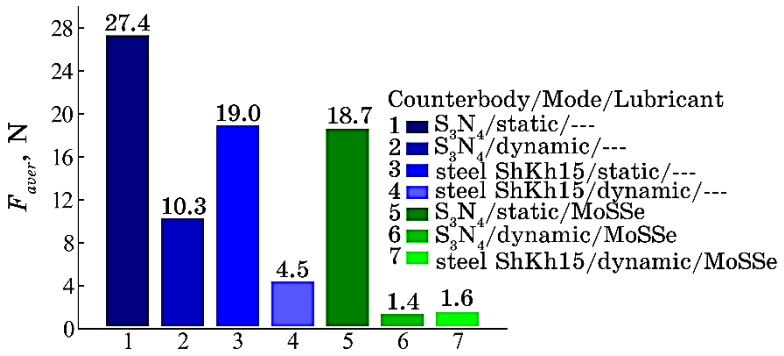

Fig. 10. Mean force of friction (F) of Si_3N_4–TiN before and after deposition of the 2*D* MoSSe solid lubricant.

reduction for the steel indenter and 2–10-fold reduction for the ceramic indenter, depending on the sliding time (Fig. 9).

These results clearly emphasize the importance of controlling adhesive interactions of the materials of the friction couple [35]. On the whole, the obtained results testify to the fact that adhesive wear rather than the abrasive wear is a dominant wear mechanism. This conclusion is true for both ceramic/steel and ceramic/ceramic contacts. This is why the reduction of adhesive interaction is of critical importance for improving the tribological characteristics of the ceramic based on Si_3N_4 (Fig. 10).

4. CONCLUSIONS

A complex investigation on obtaining a tribosystem from a wear-resistant composite ceramic based on silicon nitride was performed using a modern technology for synthesis of composite powders and their consolidation and surface covered with solid lubricant of molybdenum sulphoselenide solid solution 2*D* $MoS_{2-x}Se_x$ ($x = 1$) nanostructures. Specimens of the Si_3N_4–25% TiN dense composite ceramic with a submicron granular structure, a relative density of 98%, and a microhardness of 15.7 ± 0.8 GPa were obtained by the spark plasma sintering. A solid lubricant layer of 2*D* MoSSe nanostructures was deposited on the surface of the ceramic specimens by ultrasound-assisted deposition in ethanol.

The tribotechnical characteristics of the obtained Si_3N_4–TiN composite in couples with a ceramic and a steel counterbody under dry friction conditions and after introduction of the 2*D* MoSSe solid lubricant into the tribocontact region were determined. It was established that the introduction of the 2*D* MoSSe lubricant interlayer promotes the formation of a tribofilm and substantially reduc-

es the linear wear under static and dynamic loading conditions (by a factor of 20 and 10–11, respectively). At the same time, the solid lubricant reduced the friction forces under dynamic loading conditions by a factor of 2–6 for the steel indenter and by a factor of 2–10 for the ceramic indenter. The obtained results demonstrate that the tribofilm based on 2*D* MoSSe nanostructures forms more readily under dynamic loading for the ceramic/steel couple, which corresponds to the conditions of hybrid bearings. The obtained results create prerequisites for using developed materials in hybrid bearings and other friction units operating under extreme conditions.

ACKNOWLEDGMENTS

The authors of the paper R. V. Lytvyn, I. V. Kud, N. B. Konih-Ettel, L. I. Kulikov, O. B. Zgalat-Lozynskyy note that the presented investigations were performed with support of the National Research Foundation of Ukraine, project No. 2023.04/0046 'New lubricant additives of 2*D*-nanostructures of solid solutions of transition metal dichalcogenides for the modification of ceramic and hybrid bearings for aviation equipment'.

The authors thank Dr. Lev Axelrud from the Ivan Franko National University of Lviv, Ukraine, for the x-ray analysis.

REFERENCES

1. P. Švec, A. Brusilová and J. Kozánková, *Materials Engineering*, **16**, No. 1: 34 (2008).
2. M. Belmonte, P. Miranzo, M. I. Osendi, and J. R. Gomes, *Wear*, 266, Nos. 1–2: 6 (2009); https://doi.org/10.1016/j.wear.2008.05.004
3. B. Su, C. Lu, and C. Li, *Machines*, **12**, No. 8: 510 (2024); https://doi.org/10.3390/machines12080510
4. V. G. Kolesnichenko, O. B. Zgalat-Lozinskii, V. T. Varchenko, M. Herrmann, and A. V. Ragulya, *Powder Metall Met. Ceram.*, **53**, Nos. 11–12: 680 (2015); https://doi.org/10.1007/s11106-015-9663-1
5. O. Zgalat-Lozynskyy, I. Kud, L. Ieremenko, L. Krushynska, D. Zyatkevych, K. Grinkevych, O. Myslyvchenko, V. Danylenko, S. Sokhan, and A. Ragulya, *Journal of the European Ceramic Society*, **42**, No. 7: 3192 (2022); https://doi.org/10.1016/j.jeurceramsoc.2022.02.033
6. K. Adachi, K. Hokkirigawa, and K. Kato, *Wear*, **151**, No. 2: 291 (1991); https://doi.org/10.1016/0043-1648(91)90256-T
7. O. Zgalat-Lozynskyy, V. Varchenko, N.I. Tischenko, A. Ragulya, M. Andrejczuk, and A. Polotai, *Tribology International*, **91**: 85 (2015); https://doi.org/10.1016/j.triboint.2015.06.027
8. I. Schulz, M. Herrmann, I. Endler, I. Zalite, B. Speisser, and J. Kreusser, *Lubrication Science*, **21**, No. 2: 69 (2009); https://doi.org/10.1002/ls.72
9. M. Herrmann, Z. Shen, I. Schulz, Hu. Jianfeng, and B. Jancar, *Journal of*

Materials Research, **25**, No. 12: 2354 (2010); https://doi.org/10.1557/jmr.2010.0313
10. O. Zgalat-Lozynskyy, A. Ragulya, M. Herrmann, M. Andrzejczuk, and A. Polotai, *Archives of Metallurgy and Materials*, **57**, No. 3: 853 (2012); https://doi.org/10.2478/v10172-012-0093-5
11. F. Gutierrez-Mora, A. Erdemir, K. C. Goretta, and J. L. Routbort, *Tribology Letters*, **18**, No. 2: 231 (2005); https://doi.org/10.1007/s11249-004-2747-6
12. O. Zgalat-Lozynskyy, M. Andrzejczuk, V. Varchenko, M. Herrmann, A. Ragulya, and A. Polotai, *Materials Science and Engineering: A*, **606**: 144 (2014); https://doi.org/10.1016/j.msea.2014.03.109
13. V. G. Kolesnichenko, V. P. Popov, O. B. Zgalat-Lozinskii, L. A. Klochkov, T. F. Lobunets, A. I. Raichenko, and A. V. Ragulya, *Powder Metall Met. Ceram.*, **50**, No. 157: 11106 (2011); https://doi.org/10.1007/s11106-011-9313-1
14. J. Tatami, E. Kodama, H. Watanabe, H. Nakano, T. Wakihara, K. Komeya, T. Meguro, and A. Azushima, *Journal of the Ceramic Society of Japan*, **116**, No. 1354: 749 (2008); https://doi.org/10.2109/jcersj2.116.749
15. O. B. Zgalat-Lozynskyy, L. I. Ieremenko, I. V. Tkachenko, K. E. Grinkevich, S. E. Ivanchenko, A. V. Zelinskiy, G. V. Shpakova, and A.V. Ragulya, *Powder Metall Met. Ceram.*, **60**, No. 9: 597 (2022); https://doi.org/10.1007/s11106-022-00272-2
16. K. Holmberg and A. Erdemir, *Friction*, **5**, No. 3: 263 (2017); https://doi.org/10.1007/s40544-017-0183-5
17. B. R. Manu, A. Gupta, and A. H. Jayatissa, *Materials*, **14**, No. 7: 1630 (2021); https://doi.org/10.3390/ma14071630
18. M. Samadi, *Nanoscale Horiz.*, **3**, No. 2: 90 (2018); https://doi.org/10.1039/C7NH00137A
19. D. Berman, A. Erdemir, and A. V. Sumant, *ACS Nano*, **12**, No. 3: 2122 (2018); https://doi.org/10.1021/acsnano.7b09046
20. D. Berman, S. A. Deshmukh, S. K. R. S. Sankaranarayanan, A. Erdemir, and A. V. Sumant, *Science*, **348**, No. 6239: 1118 (2015); https://doi.org/10.1126/science.1262024
21. Y. Meng, J. Xu, Z. Jin, B. Prakash, and Y. Hu, *Friction*, **8**, No. 2: 221 (2020); https://doi.org/10.1007/s40544-020-0367-2
22. H. Li, J. Wang, S. Gao, Q. Chen, L. Peng, K. Liu, and X. Wei, *Adv. Mater.*, **29**, No. 27: 1701474 (2017); https://doi.org/10.1002/adma.201701474
23. R. Lytvyn, I. Kud, O. Myslyvchenko, R. Medyukh, L. Krushynska, and O. Zgalat-Lozynskyy, *Int. J. Appl. Ceram. Tec.*, **21**, No. 4: 2596 (2024); https://doi.org/10.1111/ijac.14683
24. I. V. Kud, L. I. Ieremenko, L. A. Krushynska, D. P. Zyatkevych, O. B. Zgalat-Lozynskyi, and O. V. Shyrokov, *Nanooptics and Photonics, Nanochemistry and Nanobiotechnology, and Their Applications. Springer Proc. in Physics* (2020), vol. **247**, p. 23; https://doi.org/10.1007/978-3-030-52268-1_2
25. O. Zgalat-Lozynskyy, M. Herrmann, and A. Ragulya, *J. Europ. Ceram. Soc*, **31**, No. 5: 809 (2011); https://doi.org/10.1016/j.jeurceramsoc.2010.11.030
26. L. M. Kulikov, N. B. Konig-Ettel, L. Yu. Matzui, A. P. Naumenko, T. A. Len, I. V. Ovsiienko, and V. I. Matzui, *Nanophysics, Nanomaterials, Interface Studies, and Applications. Springer Proc. in Physics* (2017), vol. **195**, p. 845; https://doi.org/10.1007/978-3-319-56422-7_65

27. L. Akselrud and Y. Grin, *Journal of Applied Crystallography*, **47**, No. 2: 803 (2014); https://doi.org/10.1107/S1600576714001058
28. J. Yao, Y. Wu, J. Sun, J. Tian, P. Zhou, Z. Bao, Z. Xia, and L. Gao, *Materials Research Express*, **8**, No. 3: 035701 (2021); https://doi.org/10.1088/2053-1591/abe8ab
29. D. A. Lesyk, S. Martinez, B. N. Mordyuk, V. V. Dzhemelinskyi, A. Lamikiz, G. I. Prokopenko, M. O. Iefimov, and K. E. Grinkevych, *Wear*, **462–463**: 203494 (2020); https://doi.org/10.1016/j.wear.2020.203494
30. D. A. Lesyk, S. Martinez, B. N. Mordyuk, V. V. Dzhemelinskyi, A. Lamikiz, G. I. Prokopenko, Yu. V. Milman, and K. E. Grinkevych, *Surface and Coatings Technology*, **328**: 344 (2017); https://doi.org/10.1016/j.surfcoat.2017.08.045
31. B. N. Mordyuk, G. I. Prokopenko, Yu. V. Milman, M. O. Iefimov, K. E. Grinkevych, A. V. Sameljuk, and I. V. Tkachenko, *Wear*, **319**, Nos. 1–2: 84 (2014); https://doi.org/10.1016/j.wear.2014.07.011
32. R. J. Yeo, N. Dwivedi, L. Zhang, Z. Zhang, C. Y. H. Lim, S. Tripathy, and C. S. Bhatia, *Nanoscale*, 9, No. 39: 14937 (2017); https://doi.org/10.1039/C7NR03737F
33. R. V. Lytvyn, K. E. Grinkevich, O. M. Myslyvchenko, I. V. Trachenko, O. M. Bloschanevych, S. E. Ivanchenko, O. V. Derev'yanko, A. I. Stegniy, V. D. Belik, and O. B. Zgalat-Lozynskyy, *Powder Metall Met. Ceram.*, **62**, No. 9: 611 (2024); https://doi.org/10.1007/s11106-024-00421-9
34. M. V. Zamula, A. V. Derevyanko, V. G. Kolesnichenko, O. B. Zgalat-Lozinskii, and A. V. Ragulya, *Powder Metall Met. Ceram.*, **54**, No. 1: 1537 (2015); https://doi.org/10.1007/s11106-015-9673-z
35. K. Grinkevych, O. Zgalat-Lozynskyi, N. Konih-Ettel, S. Dudka, I. Kud, S. Kyryliuk, E. Mucoz-Cortés, and R. Nevshupa, *Tribology International*, **212**: 110913 (2025); https://doi.org/10.1016/j.triboint.2025.110913